



Universiteit  
Leiden  
The Netherlands

## Evolution of clouds in radio galaxy cocoons

Mellema, G.; Kurk, J.D.; Röttgering, H.J.A.

### Citation

Mellema, G., Kurk, J. D., & Röttgering, H. J. A. (2002). Evolution of clouds in radio galaxy cocoons. *Astronomy And Astrophysics*, 395, L13-L16. Retrieved from <https://hdl.handle.net/1887/7375>

Version: Not Applicable (or Unknown)

License: [Leiden University Non-exclusive license](#)

Downloaded from: <https://hdl.handle.net/1887/7375>

**Note:** To cite this publication please use the final published version (if applicable).

# Evolution of clouds in radio galaxy cocoons

G. Mellema, J. D. Kurk, and H. J. A. Röttgering

Sterrewacht Leiden, PO Box 9513, 2300 RA, Leiden, The Netherlands

Received 31 July 2002 / Accepted 6 September 2002

**Abstract.** This letter presents a numerical study of the evolution of an emission line cloud of initial density  $10 \text{ cm}^{-3}$ , temperature  $10^4 \text{ K}$ , and size 200 pc, being overtaken by a strong shock wave. Whereas previous simple models proposed that such a cloud would either be completely destroyed, or simply shrink in size, our results show a different and more complex behaviour: due to rapid cooling, the cloud breaks up into many small and dense fragments, which can survive for a long time. We show that such rapid cooling behaviour is expected for a wide range of cloud and shock properties. This process applies to the evolution of emission line clouds being overtaken by the cocoon of a radio jet. The resulting small clouds would be Jeans unstable, and form stars. Our results thus give theoretical credibility to the process of jet induced star formation, one of the explanations for the alignment of the optical/UV and radio axis observed in high redshift radio galaxies.

**Key words.** galaxies: jets – galaxies: high redshift – galaxies: active – galaxies: evolution – cosmology: early Universe

## 1. Introduction

Regions of luminous optical line and continuum emission near high redshift radio galaxies ( $z > 0.6$ ) are often found to be extended along the direction of the radio axis (Chambers et al. 1987; McCarthy et al. 1987). One obvious explanation for these alignments is that star formation takes place in regions where the shock bounding the radio jet, has passed.

Recent observations seem to support this idea. Deep spectra of the radio galaxy 4C41.17 at  $z = 3.8$ , show that the bright, spatially extended rest-frame UV continuum emission is unpolarized and contains P Cygni-like absorption features, indicating the presence of a large population of young, hot stars (Dey et al. 1997). Bicknell et al. (2000) argue that this can best be understood if the shock associated with the radio jet has triggered star formation within the emission line clouds.

A nearby example where stars might be formed under the influence of a radio source is the case of Cen A. Here, young stars are found near filaments of ionized gas in a radio lobe (Mould et al. 2000).

Rees (1989) and Begelman & Cioffi (1989) analytically explored the evolution of intergalactic medium (IGM) clouds, overtaken by shocks from the cocoon of a radio jet. They argue that these clouds would be compressed and then gravitationally contract to form stars. However, Icke (1999) claimed that the destructive aspects of the interaction between the expanding cocoon and the clouds would dominate the evolution of the clouds. In his scenario the clouds evaporate and their material mixes into the jet cocoon.

Given the complexity of the interaction between the clouds and the jet cocoon, numerical studies are a good tool to investigate this problem. Although the “shock-cloud interaction” problem was studied numerically before, none of these studies addresses the effects of radiative cooling, important for intergalactic clouds. Here we present new results of a numerical hydrodynamic study of the shock-cloud interaction problem, including the effects of radiative cooling.

In Sect. 2 we describe the general problem of shock-cloud interaction and the application to IGM clouds. Section 3 deals with the numerical method, and Sect. 4 contains the results, which we further discuss in the fifth section. We sum up the conclusions in Sect. 6.

## 2. Shock-cloud interactions

Many numerical studies of single shock-cloud interactions have been carried out, Woodward (1976) being one of the first. Various others followed, of which we will only mention two more recent studies: Klein et al. (1994), who provided a thorough analysis of the problem, and Poludnenko et al. (2002), who studied the case of a shock running over a system of clouds; see these two papers for an overview of the literature. It is notable that in nearly all numerical studies to date, radiative cooling was either neglected or had little effect. For work considering the large scale effects of the passage of radio jets, see Steffen et al. (1997) and Reynolds et al. (2001).

The evolution of a single, non-cooling cloud, which is run over by a strong shock wave, consists of three phases. Initially, the shock runs over the cloud. The time scale for this is the shock passing time,  $t_{\text{sp}} = 2R_{\text{cl}}/v_{\text{shock}}$ , where  $R_{\text{cl}}$  is the cloud radius, and  $v_{\text{shock}}$  the velocity of the passing shock.

Send offprint requests to: G. Mellema,  
e-mail: mellema@strw.leidenuniv.nl

The second phase is the compression phase, in which the cloud finds itself inside the high pressure cocoon. It is now underpressured compared to its environment, and shock waves start to travel into the cloud from all sides. This phase lasts for a time  $t_{cc} = R_{cl}/v_{s,cl}$ , the cloud crushing time, where  $v_{s,cl}$  is the velocity of the shock travelling into the cloud. For a strong shock this velocity is of order  $v_{s,cl} = v_{shock}/\sqrt{\chi}$ , in which  $\chi$  is the ratio of the  $n_{cl}$  to  $n_{env}$ , the densities of the cloud and the environment, respectively; see Klein et al. (1994) for a better estimate.

The third phase starts when the shocks travelling into the cloud, meet and interact. This produces a rarefaction wave travelling through the shocked cloud material. The cloud, which was compressed by the shock waves, now starts expanding again, and soon afterwards is destroyed and mixes in with the surrounding flow. This typically happens in a few cloud crushing times.

### 2.1. Cloud properties

Following Rees (1989), Begelman & Cioffi (1989), and McCarthy (1993), we assume the undisturbed clouds to be the cooler and denser phase of an ionized two-phase IGM, of which the low density phase has a temperature of  $T_{ig} = 10^7$  K and a density of  $n_{ig} = 10^{-2} \text{ cm}^{-3}$ . Assuming pressure equilibrium between the two phases, a cloud temperature of  $10^4$  K gives a density of  $n_{cl} = 10 \text{ cm}^{-3}$ . We choose an initial radius of  $3 \times 10^{20}$  cm ( $\sim 100$  pc) and hence the cloud mass is  $9.5 \times 10^5 M_{\odot}$ . Following the analysis of Cygnus A by Begelman & Cioffi (1989), we take the Mach number of the shock bounding the jet cocoon to be 10, yielding  $v_{shock} = 3500 \text{ km s}^{-1}$  ( $0.01c$ ). With these parameters we obtain  $t_{sp} = 5 \times 10^4$  years,  $t_{cc} = 8 \times 10^5$  years, and  $v_{cl,s} = 120 \text{ km s}^{-1}$ .

The cooling time can be estimated from  $t_{cool} = Cv_{s,cl}^3/\rho_{cl}$  (see e.g. Kahn 1976), where  $C$  is a constant depending on the cooling processes, with a value of  $6.0 \times 10^{-35} \text{ g cm}^{-6} \text{ s}^4$  for a gas in collisional ionization equilibrium at solar abundances. With the numbers above one finds  $t_{cool} = 2 \times 10^2$  years. This is the shortest time scale thus far, showing that cooling will dominate the evolution of the shocked cloud.

It is instructive to derive a condition for which cooling will dominate. Using the expressions for  $t_{cc}$  and  $t_{cool}$ , we find that the condition  $t_{cc} > 10t_{cool}$  can be rewritten as

$$M_{cl} > 10^{-9} M_{\odot} \times \left( \frac{v_{shock}}{10^3 \text{ km s}^{-1}} \right)^{12} \left( \frac{\chi}{10^3} \right)^{-8} \left( \frac{n_e}{10^{-2} \text{ cm}^{-3}} \right)^{-2}. \quad (1)$$

This shows that cooling dominates for a large range of values for  $M_{cl}$ ,  $v_{shock}$ ,  $\chi$ , and  $n_e$ . For our values of  $M_{cl}$  and  $n_e$ , the shock velocity needs to be above  $17\,000 \text{ km s}^{-1}$ , or the density ratio  $\chi$  below 15, for cooling *not* to dominate the evolution.

### 3. Numerical method

The calculations were performed with a two-dimensional hydrodynamics code based on the Roe solver method, an approximate Riemann solver (Roe 1981; Eulderink & Mellema 1995).

Second order accuracy was achieved with the *superbee* flux limiter, which was made less steep by lowering the coefficients from 2.0 to 1.2; taking 1.0 would correspond to using the *minmod* flux limiter, see Sect. 20.2 in Laney (1998). Better two-dimensional behaviour was implemented by using the transverse waves method as described by LeVeque (1997).

In order to include the effects of cooling, we used a cooling curve (Dalgarno & McCray 1972), which gives the cooling as a function of temperature, for a low density plasma in collisional ionization equilibrium. This is a reasonable approximation of the real cooling processes of astrophysical gases. The radiative terms were implemented using operator splitting, where the appropriate radiative losses and gains were added as a separate source term every time step. The heating rate is proportional to the density, and was set so that for the initial conditions, heating and cooling in the cloud are balanced.

In order to deal with short cooling times, we subdivided the time steps into smaller fractions of the order of the cooling time when applying the cooling. We imposed a minimum temperature of 10 K. This approximately corresponds to the cosmic microwave background temperature at the redshifts we are considering. We did not follow the ionization state of the gas, but assumed the material to always be in collisional ionization equilibrium.

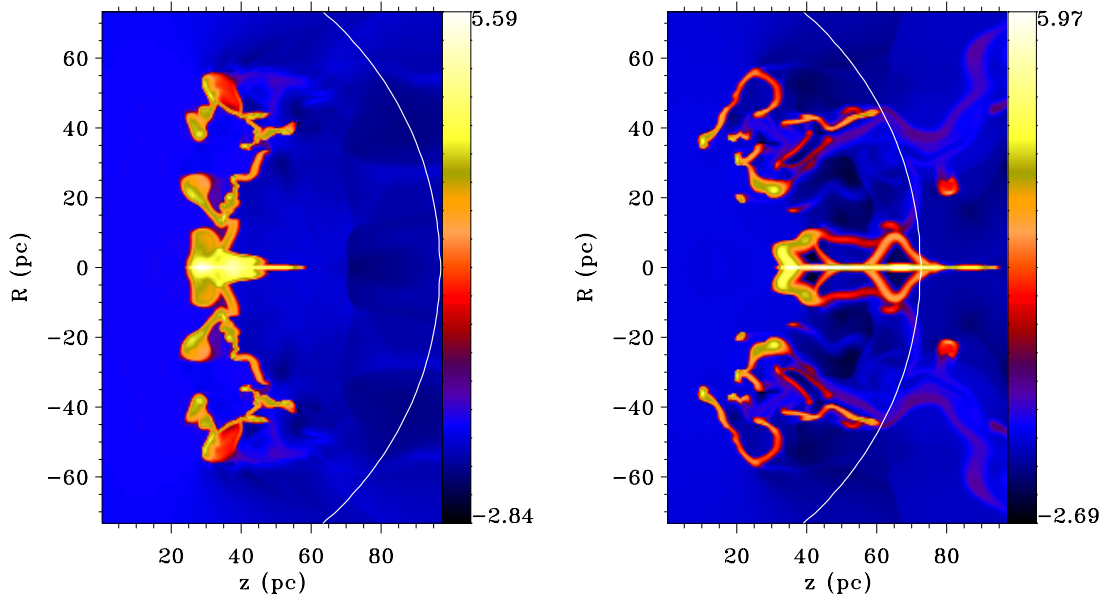
The geometry of the grid was either cylindrical ( $R, z$ ), assuming cylindrical symmetry, or cartesian ( $x, y$ ), assuming slab symmetry. The use of two different coordinate systems helps in understanding the true three-dimensional nature of the flow. Cylindrical coordinates are the proper choice as long as the flow pattern retains its large scale character, i.e. during the initial phase of the interaction. However, when the cloud starts to fragment, off-axis pieces are represented by ring-shaped structures. Furthermore, there is a strictly imposed symmetry axis at the centre of the cloud. In Cartesian coordinates the initial conditions do not describe a spheroid, but rather a cylinder. On the other hand, the fragmentation is more properly followed, and no symmetry axis is imposed.

We ran two simulations: in run A the shock wave interacted with a spherical cloud (with the parameters from Sect. 2.1) on cylindrical coordinates, and in run B with an elliptical cloud (with a semi-major axis of 100 pc, axis ratio 1.5, the major axis at an angle of  $45^\circ$  with respect to the incoming shock, and all other properties the same as in run A) on Cartesian coordinates. Using an elliptical cloud, rather than a spherical cloud, further reduces the symmetry. For both runs the cell sizes were  $0.486 \times 0.486$  pc, using  $800 \times 1600$  (A) and  $1600 \times 1600$  (B) computational cells.

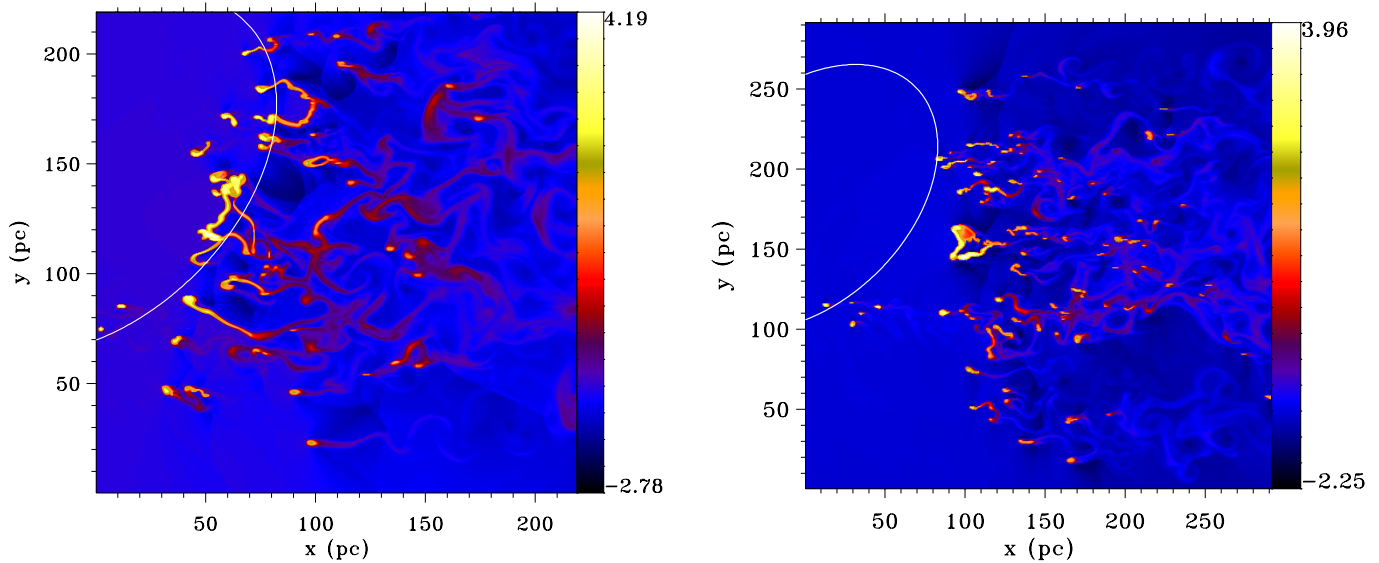
### 4. Results of the simulations

Figure 1 shows the logarithm of the density for run A at times  $0.79 \times 10^6$  and  $1.1 \times 10^6$  years. Figure 2 shows the same for run B<sup>1</sup>. The cocoon shock wave came from the left, and passed the entire cloud at  $t = 5 \times 10^4$  years.

<sup>1</sup> Movies of the entire density evolution of the two runs are available with the electronic version of this letter, at <http://www.edpsciences.org>



**Fig. 1.** Colour plots of  $\log_{10}$  of the number density ( $\text{cm}^{-3}$ ) at  $t = 0.79 \times 10^6$  years (left), and  $t = 1.1 \times 10^6$  years (right) for run A (cylindrical coordinates, spherical cloud). The white contour indicates the original cloud position. Only a fraction of the computational domain is shown. The coordinates are relative to the lower left corner of each frame. The shock wave came from the left.



**Fig. 2.** As Fig. 1 for run B (Cartesian coordinates, elliptical cloud).

At  $t = 0.79 \times 10^6$  years the shock waves travelling into the cloud have just merged (compare with the estimate for  $t_{cc}$  in Sect. 2.1). In the non-cooling case this is followed by a re-expansion of the shocked cloud (due to the extra heating generated in the merging of the shocks), but here the excess energy is radiated away, and the merging of the front- and back-side shocks leads to the formation of a dense, cool, elongated, but fragmented structure (“sheet”) perpendicular to the flow direction in run A, and more parallel to the major axis orientation in run B. In both cases there is a concentration near the centre of the former cloud.

The two righthand boxes of Figs. 1 and 2 show how this sheet fragments further. In run A, the imposed symmetries lead to an elongated concentration of material on the axis, which we

measured to contain approximately 10% of the original cloud mass. The rest of the cloud material is compressed into dense structures, spread out over a volume which is 30% of the original cloud size (part of the outer contour of the original cloud boundary is indicated in Fig. 1).

In run B the cloud develops into an ensemble of dense small fragments, filling an area of approximately the same diameter as the original cloud. Without imposing symmetry, the largest and densest fragment is found near the centre of the ensemble. The integrated density of this largest fragment was measured to be some 30% of the integrated density of the original cloud.

In both runs, at the end of the simulation, less than a percent of the original cloud material has been mixed into the cocoon, showing that the evaporation process is slow, as

is expected for high density contrasts. The ensemble does spatially disperse since the velocities of the fragments range from 90 to 500 km s<sup>-1</sup>, the leftmost fragments having the lowest velocities.

## 5. Discussion

The simulations presented here show a completely new behaviour compared to the scenarios presented in Rees (1989) (compression), or Icke (1999) (disruption). In our simulations, instead of being simply compressed or disrupted, the cloud breaks up into many small dense fragments, spread out over a certain volume, and which evaporate only slowly. This has not been seen in numerical simulations before. It is completely due to the introduction of cooling, which prevents the “third phase” or re-expansion (see Sect. 2).

We expect that full three-dimensional simulations will show a result lying somewhat in between what we found in runs A and B. It would definitely enhance rather than suppress the fragmentation, since there is one extra degree of freedom available for instabilities (see e.g. Xu & Stone 1995).

There are a number of processes which could work against the cooling, and hence slow down the compression. These are for example heating by the UV and X-ray photons from the AGN and the presence of a magnetic field in the clouds. Simulations of magnetized flows in three dimensions, as reported by Gregori et al. (1999), show that if the magnetic field is strong enough, it will actually enhance the fragmentation of the cloud, and presumably aid evaporation rather than compression. However, these simulations did not include the effects of cooling, so it is difficult to compare their results to ours.

Note that whenever the cooling time is substantially shorter than the cloud crushing time, we expect an evolution similar to the one above. Equation (1) shows that this holds for a wide range of cloud parameters. For example, the *interstellar* clouds from Poludnenko et al. (2002) should strongly cool, be compressed, and develop into a long-lived mass loading flow, something which these authors failed to achieve in their non-cooling simulations, where the clouds are destroyed within a few  $t_{cc}$ .

The further evolution of our fragments will be dominated by two processes: gravitational collapse, and further acceleration and erosion by the passing flow. All fragments found in our simulations will collapse under their own gravity, which makes them smaller, and even harder to disrupt and/or accelerate. As pointed out in Sect. 4, nearly all of the original cloud material ends up in these dense fragments, and would be available for star formation. This implies that the estimate for the induced star formation rate from Begelman & Cioffi (1989), is still valid. For a cloud filling factor (by volume) of  $10^{-3}$ , and a relativistic jet, they find an induced star formation rate of  $\sim 100 M_{\odot} \text{ yr}^{-1}$ , in rough agreement with the observations.

## 6. Conclusions

We have for the first time simulated the cooling dominated evolution of an intergalactic cloud which is overrun by the cocoon of a passing radio jet. Previous analytical studies conjectured

that the cloud would either be compressed, or be completely destroyed and evaporate into the cocoon. We instead find a new picture. Radiative cooling is so rapid, that nearly all of the cloud mass is compressed into many small and dense fragments with a long hydrodynamical survival time. These fragments are likely to collapse and form stars, in line with the scenario of jet induced star formation.

This type of fragmentation is expected whenever the cooling time is much shorter than the cloud crushing time. Evaluating this condition, shows this to be case for a wide range of parameters, stretching from intergalactic to interstellar conditions, see Eq. (1). The collapse-and-fragment sequence we find, may well be the way to create long lived mass loading flows inside post-shock regions (Hartquist & Dyson 1988).

These simulations are only a first step, and definitely more work is needed. In future papers we plan to explore the effects three-dimensionality and self-gravity have on the fragmentation process.

*Acknowledgements.* This work was sponsored by the National Computing Foundation (NCF) for the use of supercomputer facilities, with financial support from The Netherlands Organization for Scientific Research (NWO).

The research of GM has been made possible by a fellowship of the Royal Netherlands Academy of Arts and Sciences.

## References

- Begelman, M. C., & Cioffi, D. F. 1989, *ApJ*, 345, L21
- Bicknell, G. V., Sutherland, R. S., van Breugel, W. J. M., et al. 2000, *ApJ*, 540, 678
- Chambers, K. C., Miley, G. K., & van Breugel, W. 1987, *Nature*, 329, 604
- Dalgarno, A., & McCray, R. A. 1972, *ARA&A*, 10, 375
- Dey, A., van Breugel, W., Vacca, W. D., & Antonucci, R. 1997, *ApJ*, 490, 698
- Eulderink, F., & Mellema, G. 1995, *A&AS*, 110, 587
- Gregori, G., Miniati, F., Ryu, D., & Jones, T. W. 1999, *ApJ*, 527, L113
- Hartquist, T. W., & Dyson, J. E. 1988, *Ap&SS*, 144, 615
- Icke, V. 1999, in *The Most Distant Radio Galaxies*, ed. H. J. A. Röttgering, P. N. Best, & M. B. Lehnert (Royal Netherlands Academy of Arts and Sciences), 217
- Kahn, F. D. 1976, *A&A*, 50, 145
- Klein, R. I., McKee, C. F., & Colella, P. 1994, *ApJ*, 420, 213
- Laney, C. 1998, *Computational Gasdynamics* (Cambridge, UK: Cambridge University Press)
- LeVeque, R. 1997, *J. Comp. Phys.*, 131, 327
- McCarthy, P. J. 1993, *ARA&A*, 31, 639
- McCarthy, P. J., van Breugel, W., Spinrad, H., & Djorgovski, S. 1987, *ApJ*, 321, L29
- Mould, J. R., Ridgewell, A., Gallagher, J. S., et al. 2000, *ApJ*, 536, 266
- Poludnenko, A. Y., Frank, A., & Blackman, E. 2002, *ApJ*, 576, 832
- Rees, M. J. 1989, *MNRAS*, 239, 1P
- Reynolds, C. S., Heinz, S., & Begelman, M. C. 2001, *ApJ*, 549, L179
- Roe, P. 1981, *J. Comp. Phys.*, 43, 357
- Steffen, W., Gomez, J. L., Williams, R. J. R., Raga, A. C., & Pedlar, A. 1997, *MNRAS*, 286, 1032
- Woodward, P. R. 1976, *ApJ*, 207, 484
- Xu, J., & Stone, J. M. 1995, *ApJ*, 454, 172